Low power consumption bipolar resistive switching characteristics of ZnO-based memory devices

Jianwei Zhao (赵建伟), Fengjuan Liu (刘凤娟), Jian Sun (孙 建), Haiqin Huang (黄海琴), Zuofu Hu (胡佐富), and Xiqing Zhang (张希清)*

Key Laboratory of Luminescence and Optical Information, Ministry of Education, Institute of Opto-electronic Technology, Beijing Jiaotong University, Beijing 100044, China

**Corresponding author: xqzhang@bjtu.edu.cn*

Received March 14, 2011; accepted June 10, 2011; posted online August 5, 2011

Ag/ZnO/Pt structure resistive switching devices are fabricated by radio frequency (RF) magnetron sputtering at room temperature. The memory devices exhibit stable and reversible resistive switching behavior. The ratio of high resistance state to low resistance state can reach as high as 10^2. The retention measurement indicates that the memory property of these devices can be maintained for a long time (over 10^4 s under 0.1-V durable stress). Moreover, the operation voltages are very low, –0.4 V (OFF state) and 0.8 V (ON state). A high-voltage forming process is not required in the initial state, and multi-step reset process is demonstrated. Resistive switching device with the Ag/ZnO/ITO structure is constructed for comparison with the Ag/ZnO/Pt device.

OCIS codes: 310.0310, 203.4170.
doi: 10.3788/COL201210.013102.

With the recent development in the microelectronic industry, a new concept, the resistive random access memory (ReRAM), has attracted considerable attention in the field of storage technology[1,2]. This memory cell based on metal/insulator/metal (MIM) structure, in which resistance can be repeatedly switched between a high and a low value by applying an electric field, is a potential replacement of flash memory in next-generation non-volatile memory (NVM).

The resistive switching phenomenon has been observed in various materials, such as perovskite oxides $SrTiO_3$[3], solid electrolytes[4], and polymers[5]. However, these materials have their own notable disadvantages. For example, a solid electrolyte needs high write operation voltage, polymer is limited by low endurance, etc. Transition metal oxides (TMOs), such as ZnO, ZrO_2, NiO, TiO_2, and Al_2O_3[6–13], are extensively studied due to their simple constituent, excellent compatibility with complementary metal oxide semiconductor (CMOS) technology, and the capability for high scalability. The current-voltage (I-V) characteristics of the TMOs exhibit a large change resistance between high resistance state (HRS) and low resistance state (LRS) for logic off-state and logic on-state.

Compared with other devices, ZnO-based devices are promising candidates for binary oxide memory application, due to their low price, long retention time, and non-destructive readout. However, several reports have shown that the operation voltages are slightly higher and devices need a forming process in the initial state[7,14]. In this letter, ZnO-based memory devices with Ag electrode were fabricated by radio frequency (RF) magnetron sputtering, and the resistive switching properties were investigated. The devices showed the bipolar resistive switching behavior with operation voltage of less than 1 V and operating current of less than 25 mA, which are significantly lower than the results of Refs. [14, 15]. The non-electroforming process was obtained in our devices, which is suitable for high-density ReRAM device application. Multi-step switching processes were also observed, which can be used for multi-level memory applications.

In the fabrication of the ReRAM devices with Ag/ZnO/Pt structure, approximately 100-nm ZnO film was deposited on $Pt/Ti/SiO_2/Si$ substrates by RF magnetron sputtering at room temperature using a metallic Zn target. The device structure is shown in Fig. 1. A thin Ti layer was inserted between the layers of Pt and SiO_2/Si to enhance the adhesion of Pt electrode on Si substrate. A 100-nm Ag layer was used for the top electrodes. The electrodes with a diameter of 200 μm were deposited by RF magnetron sputtering with a metal shadow mask. A contraposition group with Ag/ZnO/ITO structure was deposited on quartz glass by RF magnetron sputtering at room temperature. The I-V characteristics were measured by adual-chamel system sourcemeter instrument (2612, keithley, USA). The cross sectional morphology was represented by a field emission scanning electron microscope (FESEM) (S-4800, Hitachi, Japan).

Figure 2 shows scanning electron microscope (SEM) image of the cross section of the fabricated ZnO/Pt structure. The laminated structure of ZnO/Pt is easily observable, and the overall thickness of the ZnO film is ∼100 nm. Moreover, ZnO growth on the top of Pt layer is characterized with conformability, and the interface of

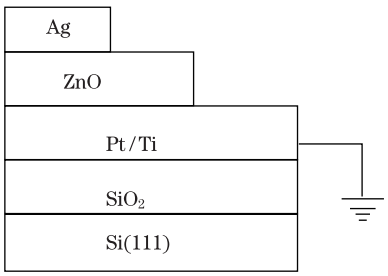

Fig. 1. Schematic structure of the designed memory stack.

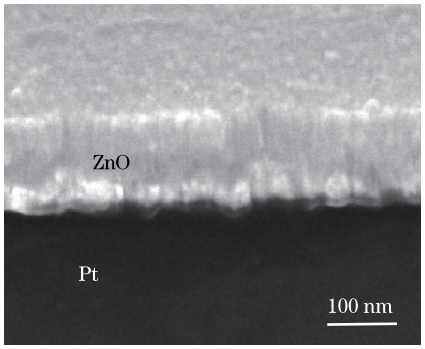

Fig. 2. Cross sectional SEM image of the interface between ZnO and Pt.

junction is touched well. The ZnO film is polycrystalline with vertical grains.

To analyze the memory performance of the Ag/ZnO/Pt structure devices, the *I-V* characteristics were investigated by direct current (DC) voltage sweeps. The characteristics are shown in Fig. 3. During the electrical measurements, the sweep voltage was applied on the Ag top electrodes (TE), while the Pt bottom electrode (BE) was grounded. A current compliance (CC) of 10 mA was adopted to avoid permanent dielectric breakdown of the devices during the SET process. The initial state of the devices exhibits high resistance of approximately $10^5\,\Omega$. In Fig. 3(a), the ReRAM devices switch to LRS (ON state) at approximately 0.8 V, when the voltage swept from zero to a positive value. When a negative sweep voltage was used, the cells reach the HRS (OFF state) at approximately −0.4 V, and the operating current is lower than 25 mA, which indicates a typical bipolar switching feature. The conductive filament formation and rupture which are controlled by electrochemical redox reaction were proposed to explain the resistive switching. Under the effect of electric field, the defects such as oxygen vacancies and Ag atoms align to form tiny conducting filaments in the HRS. These tiny conducting filaments gather together to form stronger and more conducting filaments leading to the transition to the LRS. In this process, the oxygen ions which are generated by soft excitation could be stored by the Ag TE. When DC sweep voltage from zero to negative was used, the oxygen ions which are stored in Ag TE could infiltrate the ZnO film to oxidize oxygen vacancies. This results in the rupture of conducting filament[16]. In Fig. 3(a), obvious resistance value hopping is observed both in set and reset processes, which is caused by the above mechanism. The result is different from that of other ZnO-based ReRAM devices in the reset part. This is due to the better capability of Ag electrode than that of TiN electrode in terms of adsorption and desorption of oxygen ions[17,18].

To analyze the switching behavior further, the *I-V* characteristic was plotted in a semi-logarithmic scale, as shown in Fig. 3(b). The non-electroforming process was obtained in this device, which is better than some devices which need a forming process in the initial state[19,20]. This property is beneficial in the realization of high-density ReRAM device applications in relation to laying the foundation for the preparation of large capacity memory[21]. The ratio of HRS to LRS is greater than 10^2. In the reset process, the first switching occurred at approximately −0.4 V, and the second switching took place at approximately −0.55 V. This phenomenon is produced by the devices that contain both Ag filaments and oxygen vacancy filaments. The observation is consistent with the result reported by Yang *et al.*[22]. Multi-step switching processes indicate that multi-level ReRAM devices with cache system could be obtained using the step voltage, which can effectively solve the contradiction between large capacity and high speed characteristics of memory devices.

The distributions of the set voltage and reset voltage in the case of DC voltage sweeps were measured. These are shown in Fig. 3(c). When the Ag/ZnO/Pt devices were repeatedly switched between ON and OFF states, $V_{\rm SET}$ is distributed in a range of 0.4 – 0.9 V, while $V_{\rm RESET}$ shows a narrower distribution of −0.6 – −0.3 V. The power consumption and immunity to possible electrical disturbances in the circuit are quite suitable for practical applications. Figure 3(d) shows the log-log plot and linear fitting results of the previous *I-V* curve for the positive region. The conduction mechanism in LRS could be determined by ohmic conduction. However, HRS comprises three portions: ohmic region, Child's law region, and steep current increase region. These results can be explained clearly by the typical trap-controlled space charge limited conduction (SCLC)[21,22].

Most of the researches on these memory devices have focused on the impact of the top electrode, although the effect of bottom electrode is also important. For comparison, we used indium tin oxide (ITO) instead of Pt. Figure 4 exhibits typical bipolar switching characteristic of the Ag/ZnO/ITO device. The ratio of HRS to LRS is less than 10^2, which is lower than the ratio of the Ag/ZnO/Pt device. However, the threshold voltage (SET: ∼2 V; RESET: ∼ −9 V) is higher than the latter. In the SET process, soft breakdown happens and non-lattice oxygen ions and oxygen vacancies are generated at the same time[23], which might be absorbed by the ITO electrode. Thus, when the negative sweep voltage was applied to the TE, it needed larger electric field to affect more oxygen ions detached from Ag TE to oxidize the conductive filament.

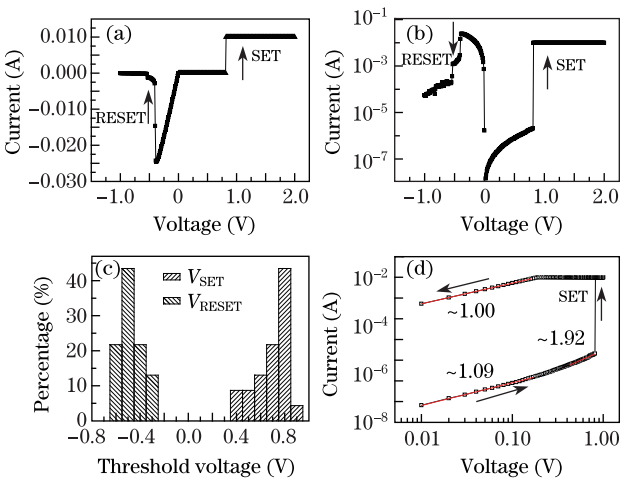

Fig. 3. Typical *I-V* characteristics of the Ag/ZnO/Pt memory device. (a) Linear scale, (b) semi-logarithmic scale, (c) distributions of SET and RESET threshold voltages, and (d) linear fitting for the *I-V* curve in log-log scale and the corresponding slopes for each portion.

Table 1. Comparison of Resistance Switching Performances Between Different ReRAM Devices

Device Structure	Forming Process	Switching Mode	Function Layer Thickness (nm)	V_{RESET} (V)	V_{SET} (V)	$R_{\mathrm{OFF}}/R_{\mathrm{ON}}$ Ratio	Retention (s)	References
Ag/ZnO/Pt	No	Bipolar	100	−0.4/−0.5	0.8	10^2	10^4	This Letter
ITO/ZnO/ITO	Yes	Unipolar	100	1.8	2.6	10^2	10^5	[7]
TiN/ZnO/Pt	No	Bipolar	30	−1.2	1.2	10^2	10^4	[17]
Al/ZrO_2/Al	Yes	Unipolar	60	0.4	2.5	10^3	–	[24]
Ag/$Zn_xCd_{1-x}S$/Pt	–	Bipolar	100	−40	40	–	–	[25]
Al/MnO_x/Pt	No	Unipolar	150	2	8	10^4	10^5	[26]

Consequently, the operation voltage was larger. However, because of the inert nature of Pt electrode, it would not react with oxygen ions. Hence, it needed lower electric field, corresponding to lower threshold voltage. Overall, the device performance of the Ag/ZnO/Pt is better than that of the Ag/ZnO/ITO.

In order to evaluate better the memory performance of the Ag/ZnO/Pt devices, the measurement of repetitive switching cycles and retention property were carried out, as shown in Fig. 5. The device was set by positive sweep voltage and reset by negative sweep voltage. Resistance values were obtained at 0.1 V. In Fig. 5(a), the values of LRS are steady within 40 switching cycles, which are distributed at approximately 20 Ω. However, fluctuated resistance values of HRS can be observed in the initial testing cycles which become relatively stable after more switching cycles, while the values are around 2 kΩ. The resistance ratio is approximately 10^2, which can meet the

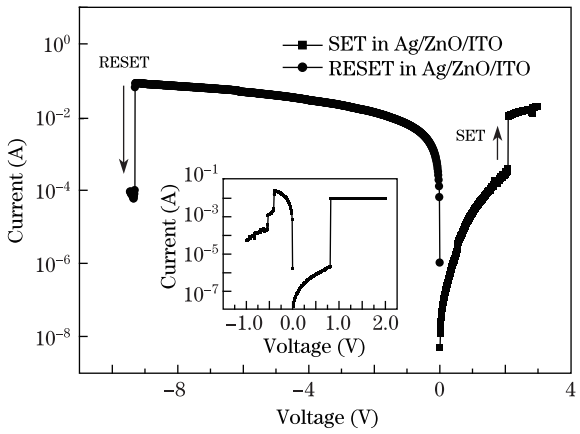

Fig. 4. Comparison of the switching characteristics of Ag/ZnO/Pt and Ag/ZnO/ITO devices. Inset shows the former device.

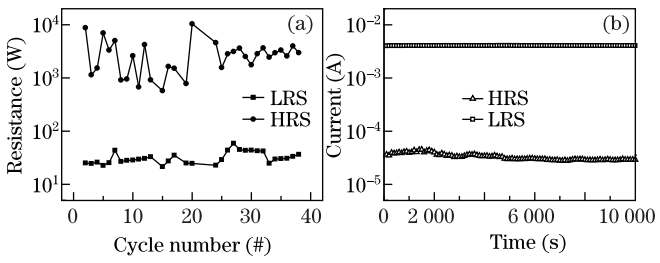

Fig. 5. (a) Switching cycling characteristics for the HRS and LRS (The resistance is measured at 0.1 V.); (b) Retention property of the resistance state at room temperature.

requirement of non-volatile memory application. Figure 5(b) shows that the resistances of both states change slightly by over 10^4 s, demonstrating the better data retention characteristic of this memory device. The negligible resistance floats of HRS and LRS at 0.1-V bias stress are possibly due to the slow polarization effect in ZnO dielectric[17].

Table 1 shows the comparison of resistance switching performances between the Ag/ZnO/Pt devices and other devices used in earlier studies. Initial electroforming process is not a requirement for the devices of the present study, which is an improvement over the results of the ITO/ZnO/ITO[7] and Al/ZrO_2/Al devices used in Ref. [24]. The ratio of HRS to LRS is approximately 10^2, which is enough for the use of memory devices. Moreover, compared with the other devices in Table 1, the operation voltage requirement is very low (<1 V). Low operation voltage means low power consumption and better stability during device use. Low operation voltage requirement can also reduce the accessories of heat dissipation, and ultimately decrease the bulk of the memory system. These have demonstrated the excellent performance of our devices for high-density integrated memory applications.

In conclusion, stable and reproducible bipolar resistive switching characteristics are achieved in the Ag/ZnO/Pt ReRAM memory devices. The low operation voltage (<1 V), low operation current (<25 mA), substantial resistance ratio (∼10^2), good retention characteristics (over 10^4 s), non-electroforming process, and multi-step reset process are demonstrated. Based on these excellent resistive switching characteristics, Ag/ZnO/Pt memory device possesses high potentiality for future non-volatile resistive switching memory applications.

This work was supported by the National Natural Science Foundation of China (No. 50972007), the Beijing Municipal Natural Science Foundation (No. 4092035), the Special Items Fund of Beijing Municipal Commission of Education, and the National Science Fund for Distinguished Young Scholars (No. 60825407).

References

1. G. I. Meijer, Science **319,** 1625 (2008).
2. R. Waser and M. Aono, Nat. Mater. **6,** 833 (2007).
3. M. Janousch, G. I. Meijer, U. Staub, B. Delley, S. F. Karg, and B. P. Andreasson, Adv. Mater. **19,** 2232 (2007).
4. H. Guo, L. Gao, Y. Xia, K. Jiang, B. Xu, Z. Liu, and J. Yin, Appl. Phys. Lett. **94,** 153504 (2009).

5. W. L. Kwan, B. Lei, Y. Shao, and Y. Yang, Curr. Appl. Phys. **10,** e50 (2010).
6. W. Guan, S. Long, Q. Liu, M. Liu, and W. Wang, IEEE Electron Device Lett. **29,** 434 (2008).
7. J. W. Seo, J.-W. Park, K. S. Lim, J.-H. Yang, and S. J. Kang, Appl. Phys. Lett. **93,** 223505 (2008).
8. K. Zheng, C. Xu, H. Zhou, M. Zhao, G. Zhu, Y. Cui, and X. Li, Chin. Opt. Lett. **7,** 238 (2009).
9. M. Zhao, G. Hu, H. Zhou, K. Zheng, G. Zhu, Y. Cui, and C. Xu, Chin. Opt. Lett. **7,** 235 (2009).
10. C. Kügeler, R. Weng, H. Schroeder, R. Symanczyk, P. Majewski, K.-D. Ufert, R. Waser, and M. Kund, Thin Solid Films **518,** 2258 (2010).
11. S. H. Chang, J. S. Lee, S. C. Chae, S. B. Lee, C. Liu, B. Kahng, D.-W. Kim, and T. W. Noh, Phys. Rev. Lett. **102,** 026801 (2009).
12. Y. H. Do, J. S. Kwak, Y. C. Bae, K. Jung, H. Im, and J. P. Hong, Thin Solid Films **518,** 4408 (2010).
13. W. Zhu, T. P. Chen, Z. Liu, M. Yang, Y. Liu, and S. Fung, J. Appl. Phys. **106,** 093706 (2009).
14. W.-Y. Chang, Y.-C. Lai, T.-B. Wu, S.-F. Wang, F. Chen, and M.-J. Tsai, Appl. Phys. Lett. **92,** 022110 (2008).
15. C.-Y. Lin, C.-Y. Wu, C.-Y. Wu, and T.-Y. Tseng, J. Appl. Phys. **102,** 094101 (2007).
16. J. Y. Son and Y. H. Shin, Appl. Phys. Lett. **92,** 222106 (2008).
17. N. Xu, L. Liu, X. Sun, C. Chen, Y. Wang, D. Han, X. Liu, R. Han, J. Kang, and B. Yu, Semicond. Sci. Technol. **23,** 075019 (2008).
18. N. Xu, L. Liu, X. Sun, X. Liu, D. Han, Y. Wang, R. Han, J. Kang, and B. Yu, Appl. Phys. Lett. **92,** 232112 (2008).
19. J.-H. Choi, S. N. Das, and J.-M. Myounga, Appl. Phys. Lett. **95,** 062105 (2009).
20. Z. Ji, Q. Maoa, and W. Ke, Solid State Commun. **150,** 1919 (2010).
21. Y. Yang, F. Pan, F. Zeng, and M. Liu, J. Appl. Phys. **106,** 123705 (2009).
22. Y. Yang, F. Pan, Q. Liu, M. Liu, and F. Zeng, Nano Lett. **9,** 1636 (2009).
23. B. Sun, Y. Liu, L. Liu, N. Xu, Y. Wang, X. Liu, R. Han, and J. Kang, J. Appl. Phys. **105,** 061630 (2009).
24. X. Wu, P. Zhou, J. Li, L. Chen, H. Lv, Y. Lin, and T. Tang, Appl. Phys. Lett. **90,** 183507 (2007).
25. Z. Wang, P. B. Griffin, J. M. Vittie, S. Wong, P. C. McIntyre, and Y. Nishi, IEEE Electron Device Lett. **28,** 14 (2007).
26. S. Zhang, S. Long, W. Guan, Q. Liu, Q. Wang, and M. Liu, J. Phys. D **42,** 055112 (2009).